Silver Nanoparticles for Conductive Ink

Subjects: Nanoscience & Nanotechnology

Contributor: Luis Llanes

Nanoparticles, defined as having one of the dimensions in the 1–100 nm range, show unique and considerably different physical, chemical, and biological properties, compared to bulk materials, due to their large portion of surface atoms and the reduced area to volume ratio.

silver nanoparticles synthesis silver-based ink formulations

1. Synthesis of silver nanoparticles （Ag NPs）

The size, shape, uniformity, and stability, as well as the corresponding physical, chemical, and biological properties of nanoparticles, are strongly dependent on synthetic methods [1]. A variety of methodologies are employed to synthesize silver nanoparticles (Ag NPs), generally classified in chemical, physical, and biological methods [2]. The different methods are described in the following sections.

1.1. Synthesis of Ag NPs by Chemical Methods

Chemical methods are the most extensively investigated route for developing Ag NPs. The chemical methods can be divided into four different categories: (1) chemical reduction, (2) electrochemical techniques, (3) pyrolysis, and (4) irradiation-assisted methods [3]. Among these methods, the chemical reduction of Ag^+ species to Ag^0 in solution using reducing agents is the most common and widely reported synthesis method of Ag NPs, usually no aggregation, high yield, and low preparation cost [2].

The formation mechanism of nanoparticles from solutions has been investigated, including nucleation and growth process [4]. The nucleation process requires more activation energy than the growth process, which is controlled by diffusion. The relative rates of nucleation and growth process are governed by varying reaction parameters, such as concentration of the reactants, the potency of the reducing agent, pH, or temperature. These parameters can be adjusted to fine-tune the nanoparticle synthesis achieving a single nucleation step and a steady growth process following a typical formation pattern of a LaMer model [5]. **Figure 1** shows a plot of the LaMer model in which the monomer concentration is shown as a function of time [6]. In Stage I, the concentration of free monomers in solution increases sharply until a supersaturation (C_s) point is obtained. The concentration of monomer is high enough to overcome the energy barrier for nucleation. In Stage II, burst nucleation leads to a significant decrease of the monomer concentration in solution, which reaches below the level of minimum supersaturation (C_{min}), where no additional nucleation occurs. In Stage III, growth continues without further nucleation to form nanocrystals. The separation of nucleation and growth process gives rise to identical growing times of all the nanoparticles, and therefore, uniformity in sizes. As an alternative to this synthesis, a very high uniformity can be achieved using seed-

mediated-growth synthesis instead of seedless synthesis. Small nanoparticles, seeds, are added to a growing solution and act as the nucleus for continuous growth. The reduction kinetics, in this case, is maintained to be slow enough not to achieve saturation.

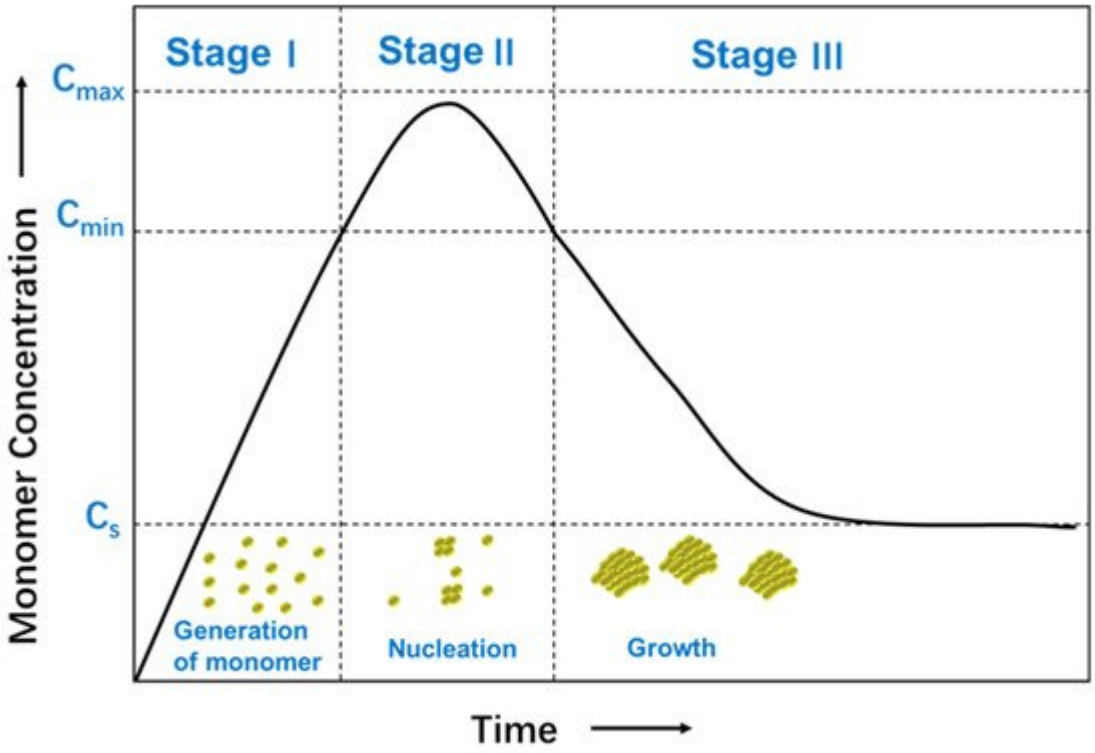

Figure 1. Schematic illustration of the LaMer model for the generation of monomers, nucleation, and subsequent growth.

The chemical reduction method usually involves three main components, i.e., metal precursors, reducing agents, and stabilizing/capping agents [7]. Different reducing agents, such as sodium citrate, ascorbate, sodium borohydride ($NaBH_4$), elemental hydrogen, polyol, Tollen's reagent, N, N-dimethylformamide (DMF), or polyethylene glycol (PEG)-block copolymers, are used. The choice of reducing agents and solvents gives rise to a different type of synthesis and offers an enormous number of possibilities.

Among the various possibilities, Turkevich's and Brust's methods, using citrate and $NaBH_4$, are the most used ones and generate very different nanoparticles in terms of sizes and solvent solubility [8][9]. Together with the choice of metal salt, reduction agent, and experimental factors, the capping agent is the main factor in determining the size and physicochemical properties of the nanoparticles [10]. This capping provides colloidal stability to the nanoparticle, either electrostatically or sterically, and controls the nanoparticle growth due to interactions with different facets, generating different morphologies. Capping agents contain polymers, such as poly (N-vinyl-2-pyrrolidone) (PVP), PEG, polymethacrylic acid (PMAA) and polymethylmethacrylate (PMMA) or small molecules such as citrate, oleilamine, alkanethiols and so on. Different morphologies (nanospheres [11], nanorods [12], nanocubes [13], nanodisks [14], nanoprims/nanotriangles [15], truncated octahedron [16], nanobipyramids [17], nanoshells [18][19], nanobars [20], nanorice [20], nanowires [21] and nanostars [22]) have been achieved by selecting

capping agents and controlling experimental parameters, as shown in **Figure 2**. The nanoparticle shape controls, among others, the plasmonic modes and offers the possibility to manipulate and respond to a light stimulus that goes from 400 nm to the middle infrared [23][24]. The morphology is also relevant in their catalytic activity and the creation of electrical paths in conductive composites and inks, where high aspect ratio morphologies are preferred.

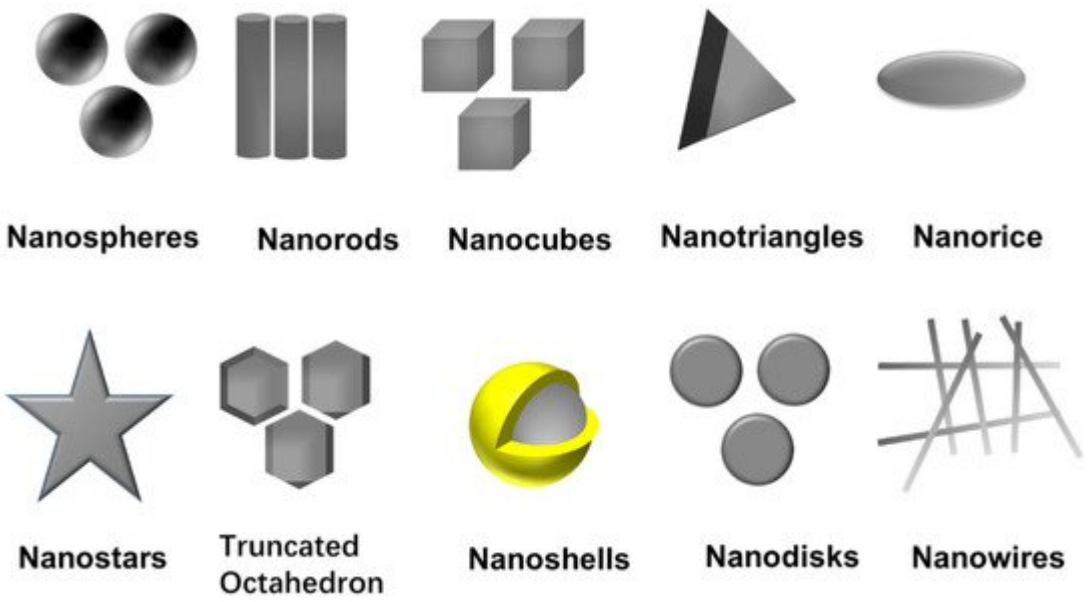

Figure 2. Ag NPs with different shapes.

The synthesis parameters (reaction temperature, pH of precursors, reducers and stabilizing agents) are crucial factors in determining nanoparticles formation and nucleation process. Many different examples of Ag NPs synthesis were proposed. Wiley et al. [25] obtained Ag NPs with three different shapes (nanocubes, bipyramids, nanowires) using ethylene glycol as a reducing agent. In their experiment, PVP was added as a stabilizing agent and reducing agent, which also played a role in controlling the shape. In addition, during the reaction, the seeds with district crystal structures were selected via etching, which produced the different morphologies of Ag NPs. Xue et al. [26] reported pH-switchable silver nanoprism growth pathways. They found that excellent control over the growth of Ag nanoprisms can be achieved by adjusting solution pH. Jiang et al. [27] investigated the reaction temperature effect on the formation and growth of Ag NPs using two or three reducing agents, including citric acid, l-ascorbic acid, and $NaBH_4$. They found that there was a significant jump in the particle size at around 32 °C. The size of plates increases from 90 to 180 nm and from 25 to 48 nm for spheres. Yoo et al. [28] synthesized Ag NPs via hydrazine reduction of Tollen's reagent. AgCl and ammonium hydroxide were mixed in the presence of PVP as a stabilizer, resulting in a clear solution without any precipitate. Then, hydrazine hydrate was injected to reduce $[Ag(NH_3)_2]^+$ and obtain Ag NPs at room temperature. The size of the obtained Ag NPs was controlled by the concentration of PVP. The diameter of Ag NPs ranged from 68 to 119 nm. In addition, AgCl was retrieved from the electronic scrap and used as a metal precursor. Zhang et al. [29] prepared colloid Ag NPs by using hyperbranched poly(methylene bisacrylamide-aminoethyl piperazine) with terminal dimethylamine groups (HPAMAM-$N(CH_3)_2$) as the effective reducing and stabilizing agent. The Ag NPs were synthesized by mixing $AgNO_3$ aqueous solution with HPAMAM-$N(CH_3)_2$ aqueous solution at room temperature. A series of Ag NPs were prepared by adjusting the

molar ratio of N/Ag in feed. Malassis et al. [30] used one-step aqueous synthesis of Ag NPs using ascorbic acid (vitamin C) as a reducing and stabilizing agent at the same time. Metal precursor, $AgNO_3$, is mixed with ascorbic acid under a strong stirring at room temperature for 30 s. It was showed that the size of Ag NPs obtained in the range of 20 to 175 nm was affected by the pH of either the metal salt solution or the ascorbic acid solution. Leng et al. [31] produced Ag NPs by the reduction of $AgNO_3$ using the ethylene glycol in the presence of PVP. They also studied the different reaction conditions (i.e., $AgNO_3$ concentration, $AgNO_3$ and PVP mass ratio and the reaction temperature) on the size and size distribution of Ag NPs. When the mass ratio of $AgNO_3$ to PVP was 2:1, Ag NPs with a narrow size distribution from 20 nm to 30 nm were obtained. Sakthivel et al. [32] prepared isonicotinic acid hydrazide capped Ag NPs by the wet chemical method and used $NaBH_4$ as a reducing agent. The synthesized Ag NPs distributed in two ranges and the average size of the particles is 35 and 536 nm. Isonicotinic acid hydrazide capped Ag NPs were applied to detect Hg^{2+} in an aqueous medium in the nanomolar range. Sreelekha et al. [33] synthesized Ag NPs using trisodium citrate as reducing and stabilizing agents via the chemical method. As described, Ag NPs were prepared by mixing the trisodium citrate solution and $AgNO_3$ solution at a temperature of about 80 °C, followed by separation of the NPs by centrifugation and drying to collect. Kamarudin et al. [34] fabricated two types of Ag NPs by varying the amount of precursor and synthesis temperature. The higher the reaction temperature, the higher the reaction rate, which increased the process of ions to NPs conversion.

Waqas et al. [35], for instance, successfully fabricated Ag NPs with three different shapes (i.e., spherical, star and pyramidal) via a simple wet chemical approach. An aqueous solution containing silver nitrate ($AgNO_3$), sodium hydroxide, oleic acid, and ammonia was used in their synthesis. During the reaction, the concentration of sodium hydroxide and oleic acid played an essential role in controlling the size, shape, and homogeneity of Ag NPs. Among all the three shapes, Ag NPs with star shape showed the highest electrocatalytic sensing efficacy in terms of linear range, the limit of detection, and sensitivity, because of more exposed catalytic active sites and fast diffusion of ions between electrode-electrolyte interfaces.

Meanwhile, Makwana et al. [36] successfully prepared fluorescent Ag NPs by only applying a single chemical regent calix [37] resorcinarene polyhydrazide (CPH) which acted as a reduction and dispersant agent. Bearing hydrazide group of CPH on its periphery acted as a reducing agent and its web type of structure as a stabilizing agent for the formation of calix-protected Ag NPs. Their results showed a large quantity of well-dispersed spherical CPH-Ag NPs with an average diameter of 7 nm. In addition, CPH-Ag NPs were not only selective and sensitive fluorescent sensors for Fe^{3+} from 0.1 to 10 μM but also exhibited reasonably good antimicrobial activity.

Bare Ag NPs are not stable and can rapidly undergo agglomeration due to their high reactivity. In most of the preparation routes, capping agents are required to control the particle size, from absorbing or attaching with each other surfaces and avoiding the aggregation of nanoparticles; coating is a way to produce electrostatic, steric or electrosteric interactions between particles and helps stabilize the nanoparticles [38][39]. Conversely, the capping agents often influence various properties of nanoparticles, including their shape and interactions with surrounding solvent, therefore, their dispersibility and size [10]. For instance, Ajitha et al. [10] investigated the influences of capping agents (PEG, ethylenediaminetetraacetic acid (EDTA), PVP, and polyvinyl alcohol (PVA)) on Ag NPs using a simple chemical reduction method. As described in their research, the average particle size was the largest for

the PEG-capped NPs with a diameter of 44 nm and the smallest for the PVA-capped ones with a diameter of 27 nm. In addition, the PVA-capped ones were observed to be the most stable and to display the highest antibacterial activity.

1.2. Synthesis of Ag NPs by Physical Methods

Physical methods usually are fast, do not involve toxic chemicals, and form a relatively narrow distribution of the synthesized Ag NPs size. However, they present several disadvantages compared with chemical methods, such as less control on the nanoparticle morphologies, more significant difficulties for the scaling and the requirement of more sophisticated equipment during the synthesis process. There are several different physical methods to synthesize Ag NPs, such as evaporation-condensation [3], ball milling [40], arc discharge [41], laser ablation [42], and pulsed wire evaporation (PWE) [43].

The PWE method is known as a one-step synthetic technique to obtain nanoparticles through evaporation and condensation processes with high efficiency and high production rate [44], as shown in **Figure 3**. In the PWE method, electrical energy with a high voltage and high electric current is applied through a thin metallic wire, resulting in the heat and evaporation of the thin wire. Then, nanoparticles can be obtained by condensation through a peripheral cooling gas or liquid. The product mass and size of nanoparticles can be controlled by changing the wire explosion number, voltage, and current [43].

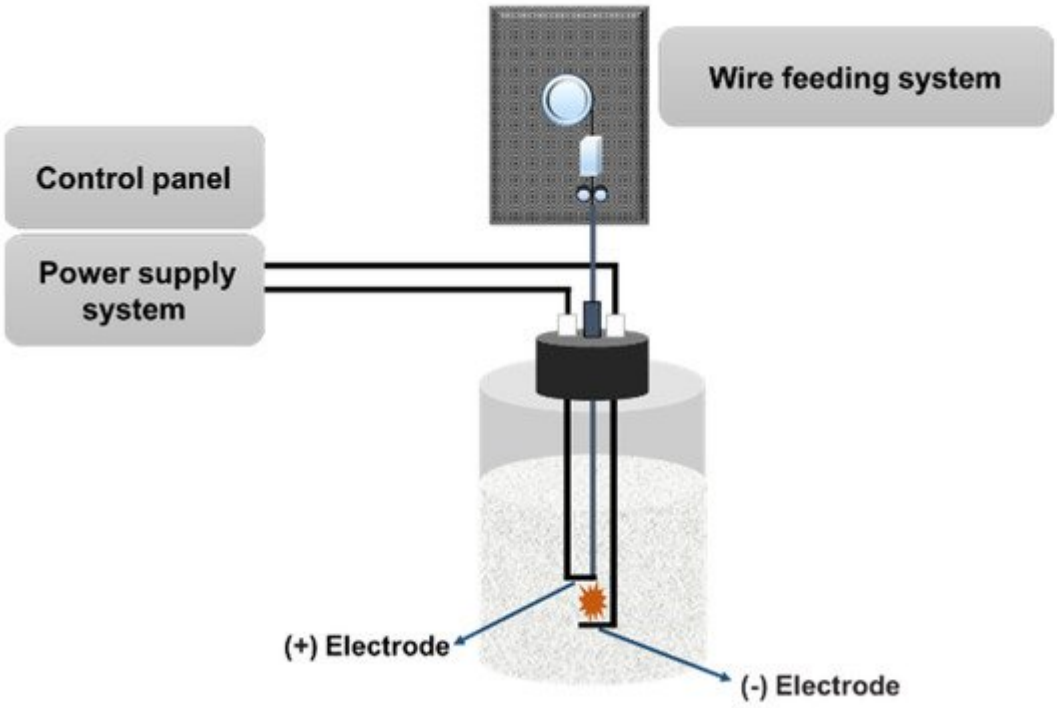

Figure 3. Schematic of PWE. In this technique, a high voltage is applied at the tip of the wire in a liquid solution, generating nanoparticles after evaporation and condensation.

Song et al. [45] investigated the effect of variation in voltage on the morphology and microstructure of Ag NPs synthesized by PWE. The average particle size increased by increasing the supply voltage without any impurity and oxide phase. The obtained Ag NPs exhibited an almost spherical shape and very small particle size (less than 30 nm). In addition, Chung et al. [46] fabricated silver/copper combined nanoparticles by one-step electrical explosion of metal wires. The silver/copper nano inks were printed on flexible polyimide (PI) and sintered via the flash white light process. The sintered films show a lower resistivity (4.06 μΩ·cm) and oxidation stability than the copper nanoparticle film.

2. Silver Inks for Printing Techniques

The typical inks used for printing methods contain functional particles (for example, Ag NPs), binders, solvents, and additives. The common strategy for the formulation of silver inks is to add silver nanomaterials into polymers dissolved in suitable solvents to fabricate conductive inks. In some cases, this polymer could be the same as the capping agent that stabilizes the nanoparticles. In order to protect Ag NPs in inks against aggregation and oxidation, organic stabilizers/polymers are required. Then, a high-temperature sintering step is often needed to remove organic stabilizers and improve the conductivity, taking into account that the temperature may affect the substrate. More recently, a novel kind of metallic inks has been developed, called reactive ink, as a low-cost and promising alternative for fabricating highly conductive silver tracks. Reactive silver ink is a pure solution-phase ink mainly composed of a silver salt precursor and complexing agent. After printing, conductive silver can be generated through a reduction reaction and /or by the decomposition of a metal-organic precursor [47].

It should be noted that different performance and properties of conductive inks should be used by different printing technologies depending on the type of printing technology being used and the desired printed performance. In this review, three printing technologies (inkjet printing, screen printing and aerosol jet printing) are discussed. The inkjet printer ejects droplets of inks as required through the printing nozzle on a variety of substrates, as shown in **Figure 4**. There are two different modes of how the droplet is jetted from the nozzle, i.e., continuous inkjet printing and drop-on-demand printing. The optimum viscosity and surface tension for inkjet printing should be in the range 0.001–0.1 Pa·s and 15–25 $mN \cdot m^{-1}$, respectively [47]. Screen printing is the process that transfers the inks to pass through the patterned stencil with a squeegee. The optimum viscosity and surface tension for inkjet printing should be in the range 0.5–5 Pa·s and 0.001–0.1 Pa·s and 38–47 $mN \cdot m^{-1}$, respectively [47]. Aerosol jet printing is the process that involves forming an ink aerosol and then spraying the aerosol onto the surface of the substrates. The aerosol jet printing technique permits working with a large range of viscosities (0.7–2500 mPa·s) and lateral resolution even below 10 μm [48].

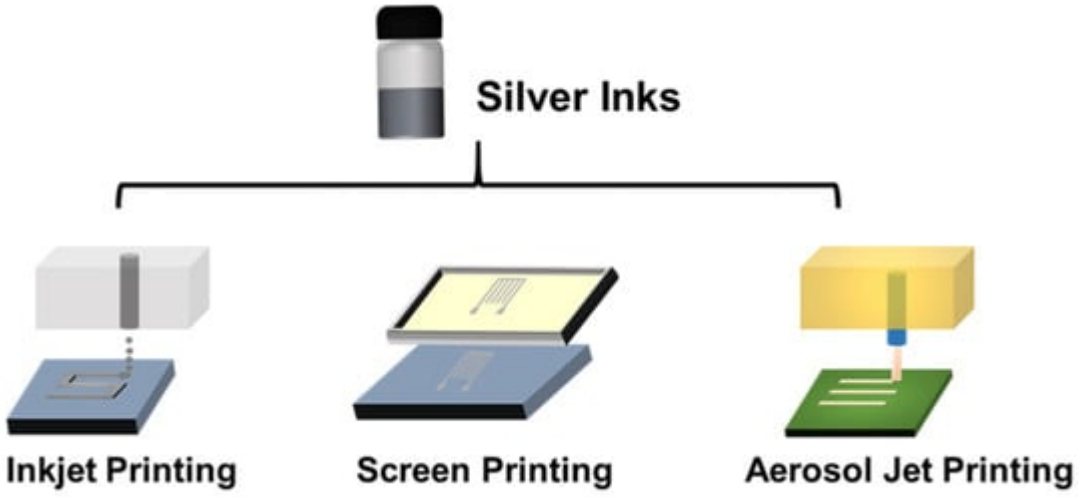

Figure 4. Schematic of inkjet printing, screen printing and aerosol jet printing.

2.1. Formulation of Silver Inks for Inkjet Printing

Typically, the inks for inkjet printing require a viscosity in the range from 0.001 to 0.1 Pa·s and surface tension from 15 to 25 $mN \cdot m^{-1}$ [47]. Therefore, during and after the Ag NPs synthesis must be taken care of fitting these recommended ranges. That is usually assured by controlling Ag NPs concentration, using a suitable solvent or additives. Cheon et al. [49] reported on the synthesis of Ag NPs for inkjet printing using electrolysis. It was showed that they could obtain Ag NPs of different sizes (10–80 nm) by controlling the applied voltage and the electrolyte temperature. The used electrolyte consisted of citric acid, hydrazine monohydrate, dispersion agent in deionized water. Kosmala et al. [50] reported on the synthesis of aqueous Ag NPs inks by a simple wet chemistry method, resulting in the formation of Ag NPs with a diameter around 50 nm. A triblock copolymer was used as Ag NPs dispersing agent and a high-intensity focus ultrasound to reduce the particle size from ~200 nm to 50 nm. Chen et al. [51] used a one-step synthesis of Ag NPs in a toluene solution containing dodecanoic acid or octadecanoic acid with the addition of n-butylamine and hydrazine, as shown in **Figure 5**. The Ag-dodecanoic acid NPs were finally suspended at 10 wt.% in cyclohexane to be employed in inkjet printing.

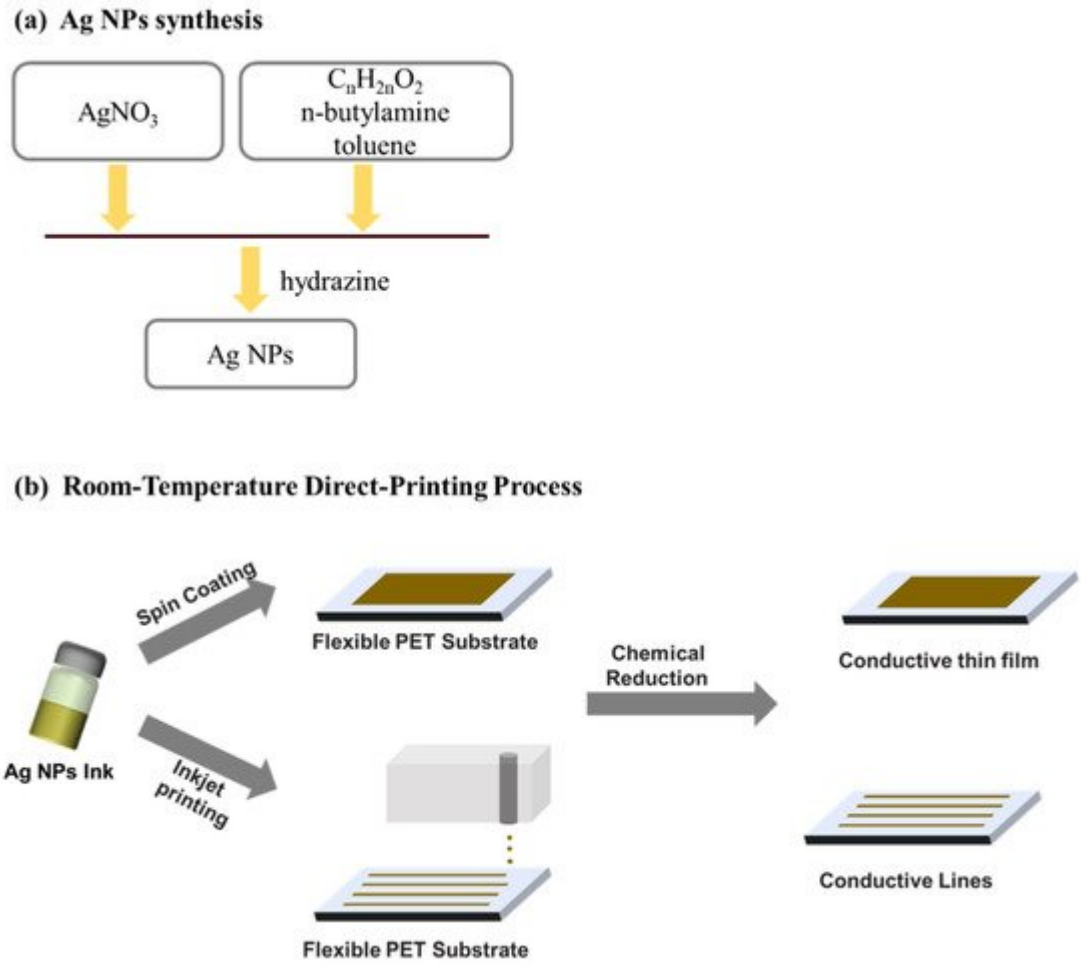

Figure 5. (**a**) Schematic illustration of the whole process of Ag NPs synthesis; and (**b**) the direct printing process.

Jung et al. [52] showed a simple way of synthesizing and sintering Ag NPs employing a simple thermal decomposition process. The Ag NPs were synthesized by simple heating and stirring of $AgNO_3$ in the presence of the surfactant (oleylamine), without a reducing agent. After dispersion and centrifugation in toluene and methanol, Ag NPs were dispersed in hexadecane at the concentration of 30 wt.%. Tung et al. [53] synthesized Ag NPs with different shapes (spherical, prism, rod, and multifaceted NPs) by variation of PVP concentration using a rapid water radiolysis approach via X-ray diffraction analysis (XRD). The resulting NPs aspect ratio from 1 up to ~50 was reached for optimized reagent concentrations. The ink concentration for inkjet printing was set to 15 wt.% in methanol. Novara et al. [54] used “in situ” reduction of silver by printing $AgNO_3$ solutions on the porous silicon surface covered with reactive hydrides. The influence of $AgNO_3$ concentration and solvents (water-ethanol, water-dimethyl sulphoxide) on the morphology of the printed Ag NPs layer were investigated. Zhang et al. [55] used a tannic acid (TA) to stabilize the synthesized Ag NPs, which resulted in an environmentally friendly approach to upscale the inkjet printable Ag NPs based inks. The Ag NPs were prepared by the employment of the silver ammonia as a silver source and TA as a reducing and capping agent simultaneously. The whole reaction was carried out in a deionized water medium at room temperature for a very short time (30 min). The formation of Ag NPs was observed by the colour changes of the solution colour from colourless to yellowish and finally dark brown. Subsequently, the Ag NPs with an average diameter of 15 nm were purified in ethanol and deionized water, and

collected by precipitation and drying. The obtained Ag NPs could be stored without oxidation for several months. Ag NPs inks at the solid content of 1–10 wt.% were prepared by dispersing different quantities of Ag NPs in deionized water. In addition, 25 vol.% of isopropanol was used to adjust the surface tension and viscosity of the ink. Conductive patterns were obtained by inkjet printing the Ag NPs inks onto photo paper. Low resistivity was achieved with sintering at 200 °C.

Liu et al. [56] showed how to synthesize bimodal Ag NPs by changing the solution temperature and concentration of $AgNO_3$. It was first synthesized Ag NPs of 10 nm in size at room temperature and $AgNO_3$ concentration of 100 $g \cdot L^{-1}$, and subsequently, larger Ag NPs of 50 nm at a boiled state and $AgNO_3$ concentration of 0.54 $g \cdot L^{-1}$. Finally, the prepared Ag NPs of the two different sizes were mixed in different ratios. The ratio of 2:1 (Ag NPs of 10 nm in size and Ag NPs of 50 nm in size) resulted in a decreased resistivity of 3.66×10^{-6} Ω·cm, with respect to each of them individually. Furthermore, the improved mechanical stability of the printed layers was also observed for this ratio.

Barrera et al. [57] synthesized Ag NPs by employing two different methods (chemical and microwave radiation). The chemical method was based on adding $AgNO_3$ into a solution of $NaBH_4$ and subsequently adding sodium citrate and PVP to stabilize the solution. The synthesis by microwave radiation was realized by mixing DMF, $AgNO_3$, and PVP in the tube of a single-mode reactor microwave under constant magnetic agitation. The Ag NPs prepared by microwave radiation were mixed with polyvinyl butyral (PVB), resulting in a nanocomposite with improved antibacterial properties with respect to Ag NPs prepared by chemical method.

Trinh et al. [58] prepared Ag NPs by chemical reduction of $AgNO_3$ using $NaBH_4$ with chitosan (CS) and cetyltrimethylammonium bromide (CTAB) as capping agents. The synthesized Ag NPs improved ink stability (more than 6 months) and cubic crystal structure with a size under 10 nm. After the synthesis, Ag NPs were mixed with glycerol, isopropanol, and deionized water to achieve the ink with appropriate viscosity and surface tension.

Another synthesis approach was used by Hao et al. [59], who applied a carboxyl-terminated hyperbranched polymer (CHBP) to stabilize the synthesized Ag NPs according to the procedure shown in **Figure 6**. The Ag NPs with almost monodisperse particles and a diameter of 10-20 nm were synthesized by chemical reduction of $AgNO_3$ using $NaBH_4$ in an aqueous phase. The final resistivity of the printed Ag NPs layers sintered at 180 °C was 10.83 μΩ·cm, which is approximately seven times higher than in case of bulk silver (1.58 μΩ·cm).

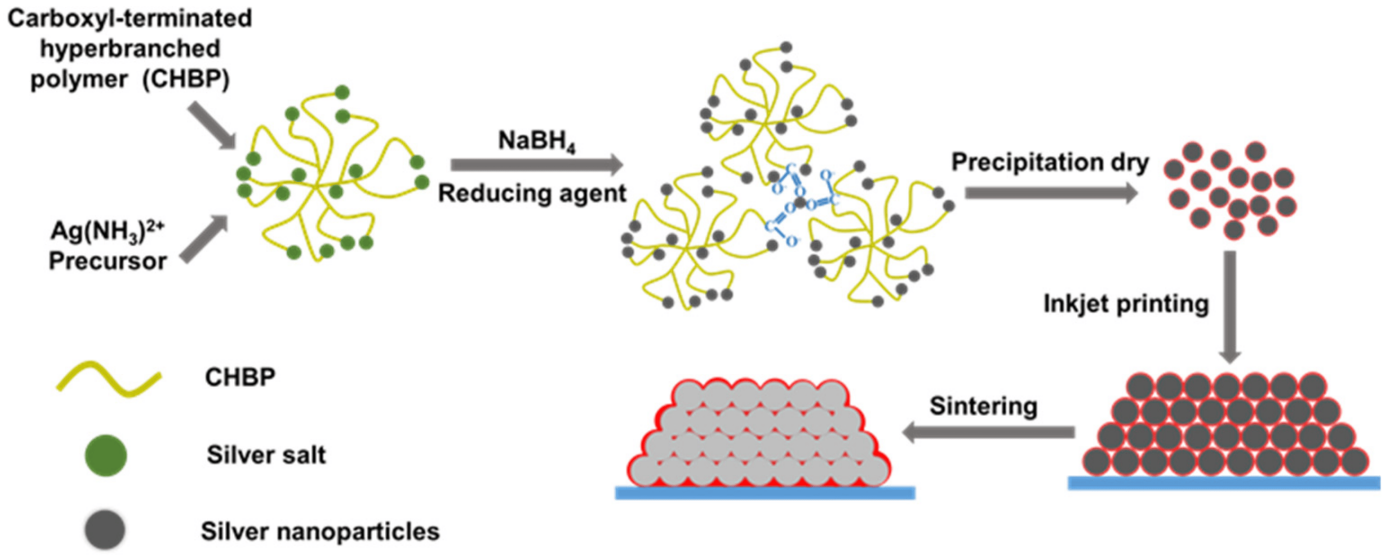

Figure 6. Schematic illustration of the CHPB stabilized Ag NPs and the process Ag NPs sintering.

Yang et al. [60] showed a simple way to prepare Ag particle-free inks, which could be a possible cheap substitute for Ag NPs based inks, as shown in **Figure 7**. The ink was prepared by simple dissolution of a silver oxalate powder in different alcohols (methanol, ethanol, butanol, hexanol and 2-methoxyethanol or a mixture of them) using 1,2-diaminopropane (1,2-DAP) as the ligand. After the printing and sintering at 180 °C, the resulting silver layer resistivity was 15.46 μΩ·cm, which is only ten times higher than that of bulk silver.

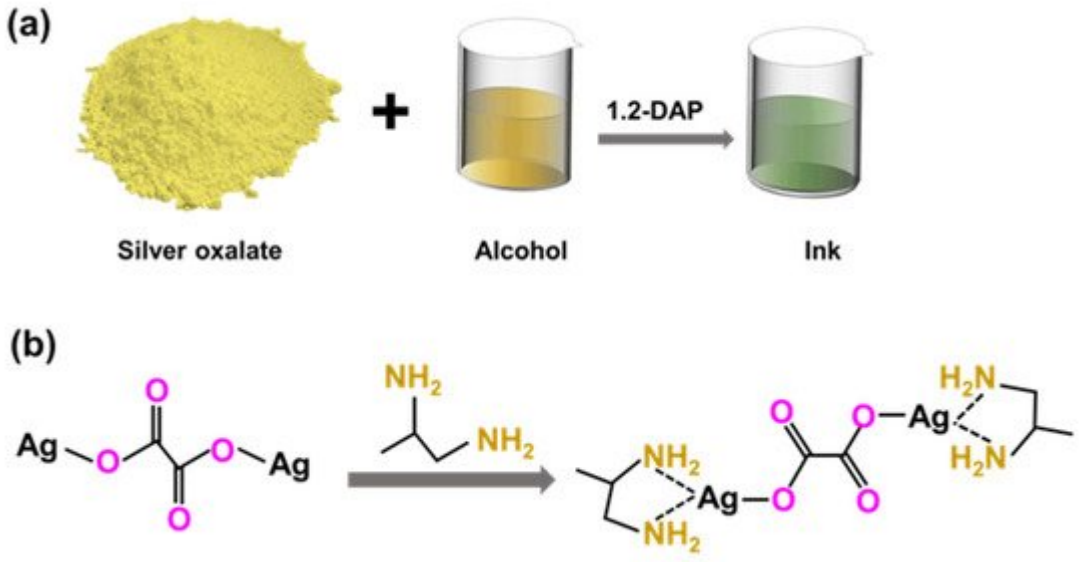

Figure 7. (**a**) Schematic illustration of the one-pot silver particle-free ink and (**b**) chemical reaction occurring during the ink synthesis.

2.2. Formulation of Silver Inks for Screen Printing

The screen printing technique typically works with viscosities ranging from 0.5 to 5 Pa·s and the surface tension from 38 to 47 $mN \cdot m^{-1}$ [47]. Therefore, to comply with such requirements, Ag NPs need to be dispersed in a suitable

polymer matrix and solvent, which assure the sufficiently high viscosity of the ink. Jadav et al. [61] used the bottom-up technique to synthesize Ag NPs, which were subsequently used to formulate a silver/silver chloride (Ag/AgCl) screen-printable ink for fabrication of electrodes for detection of vitamin C concentration from fruit juices. Epoxy resin was used as a binder combined with a commercial hardener to achieve the desirable rheologic characteristics that made it suitable for the screen printing process. Liu et al. [62], an anion-mediated synthesis was used to prepare monodisperse Ag NPs. They used $AgNO_3$ as a metal source, in combination with glucose, PVP, and different anions ($–SO_4^{2–}$, $–PO_4^{3–}$, $–CO_3^{2–}$ and $–Br^–$) to tailor the morphology of the particles. The influence of the nitrate-glucose ratio and reaction temperature on the shape and size of the synthesized Ag NPs were also investigatited. These nanoparticles were then re-dispersed in ethanol at a concentration of 30 wt.%, subsequently screen-printed onto the PET and paper substrate, and sintered at room temperature. Ding et al. [63] used a one-step polyol method to upscale the Ag NPs synthesis in ethylene glycol in the presence of PVP. The particle size (from 52 to 120 nm) was controlled by the mass ratio variation of $AgNO_3$ and PVP. Subsequently, the Ag NPs were re-dispersed in ethanol at 70 wt.% and printed in different conductive structures on PET substrate, reaching conductivities close to bulk silver, as shown in **Figure 8**.

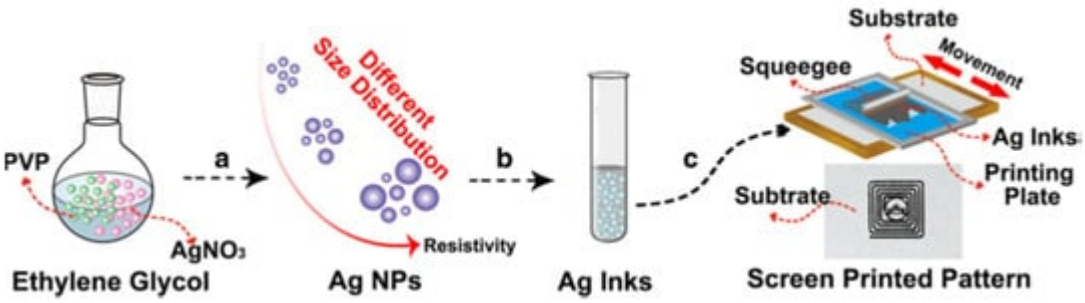

Figure 8. Schematic illustration of the whole process of screen printing Ag NP-based ink preparation from the synthesis to the printing of conductive pattern. (**a**) The preparation of Ag NPs with different size distribution; (**b**) The dispersion of Ag NPs in ethanol to form silver inks; (**c**) Screen printing of silver inks. Reprinted from Ref. [63].

2.3. Formulation of Silver Inks for Aerosol Jet Printing

The aerosol jet printing technique permits working with a large range of viscosities (0.7–2500 mPa·s) and lateral resolution even below 10 µm [48]. Salary et al. [48] also point out that aerosol jet printing is very sensitive to ink temperature and solvent evaporation rate, which may cause instabilities during the printing, such as pre-drying or particle accumulation within the printer nozzle.

Shankar et al. [64] used the non-aqueous synthesis in toluene with dodecylamine, and subsequent addition of silver acetate and a small amount of tin acetate, resulting in a formation of Ag NPs of 5–20 nm in size. The synthesized Ag NPs were then dispersed in decane and the viscosity (1–2 mPa·s) of the solution was adjusted by adding 2-buthoxyethanol at the concentration of 20 % by weight. Ivanov et al. [65] used a pulsed-periodic gas discharge in an air atmosphere to produce Ag NPs with a multigap gas-discharge generator from 99.95% purity silver. The resulting Ag NPs were then deposited by a focused aerosol beam on a glass substrate. Sonawane et al. [66] deposited branched polyethylenimine (BPEI)-functionalized Ag NPs on a substrate utilizing aerosol with flowing argon gas.

BPEI-functionalized Ag NPs were dispersed at a concentration of 0.02 mg/mL in deionized water. To create the aerosol, the solution was poured into an ultrasonic nebulizer with an additional inlet for argon gas and an outlet connected to a quartz tube, followed by the plasma treatment. After the plasma treatment, the size of the Ag NPs was reduced from 10 to 5 nm, and a well-dispersed film was formed. The plasma treatment resulted in morphological changes in Ag NPs, enhancing their optical properties. Additionally, the plasma treatment resulted in a blue shift of approximately 70 nm in the peak of the surface plasmon resonance, which is typical for the high-temperature thermal treatment. Therefore, no additional thermal sintering was necessary in this case. The desired deposition and plasma treatment can be applied to a wide range of nanoparticle systems on flexible substrates.

References

1. Nair, L.S.; Laurencin, C.T. Silver Nanoparticles: Synthesis and Therapeutic Applications. J. Biomed. Nanotechnol. 2007, 3, 301–316.
2. De Souza, T.A.J.; Souza, L.R.R.; Franchi, L.P. Silver Nanoparticles: An Integrated View of Green Synthesis Methods, Transformation in the Environment, and Toxicity. Ecotoxicol. Environ. Saf. 2019, 171, 691–700.
3. Wei, L.; Lu, J.; Xu, H.; Patel, A.; Chen, Z.-S.; Chen, G. Silver Nanoparticles: Synthesis, Properties, and Therapeutic Applications. Drug Discov. Today 2014, 20, 595–601.
4. Washio, I.; Xiong, Y.; Yin, Y.; Xia, Y. Reduction by the End Groups of Poly (Vinyl Pyrrolidone): A New and Versatile Route to the Kinetically Controlled Synthesis of Ag Triangular Nanoplates. Adv. Mater. 2006, 18, 1745–1749.
5. Togashi, T.; Tsuchida, K.; Soma, S.; Nozawa, R.; Matsui, J.; Kanaizuka, K.; Kurihara, M. Size-Tunable Continuous-Seed-Mediated Growth of Silver Nanoparticles in Alkylamine Mixture via the Stepwise Thermal Decomposition of Silver Oxalate. Chem. Mater. 2020, 32, 9363–9370.
6. LaMer, V.K.; Dinegar, R.H. Theory, Production and Mechanism of Formation of Monodispersed Hydrosols. J. Am. Chem. Soc. 1950, 72, 4847–4854.
7. Zhang, X.-F.; Liu, Z.-G.; Shen, W.; Gurunathan, S. Silver Nanoparticles: Synthesis, Characterization, Properties, Applications, and Therapeutic Approaches. Int. J. Mol. Sci. 2016, 17, 1534.
8. Dong, X.; Ji, X.; Wu, H.; Zhao, L.; Li, J.; Yang, W. Shape Control of Silver Nanoparticles by Stepwise Citrate Reduction. J. Phys. Chem. C 2009, 113, 6573–6576.
9. Oliveira, M.M.; Ugarte, D.; Zanchet, D.; Zarbin, A.J. Influence of synthetic parameters on the size, structure, and stability of dodecanethiol-stabilized silver nanoparticles. J. Colloid Interface Sci. 2005, 292, 429–435.

10. Ajitha, B.; Reddy, Y.A.K.; Reddy, P.S.; Jeon, H.-J.; Ahn, C.W. Role of Capping Agents in Controlling Silver Nanoparticles Size, Antibacterial Activity and Potential Application as Optical Hydrogen Peroxide Sensor. RSC Adv. 2016, 6, 36171–36179.
11. Lin, X.; Lin, S.; Liu, Y.; Gao, M.; Zhao, H.; Liu, B.; Hasi, W.; Wang, L. Facile Synthesis of Monodisperse Silver Nanospheres in Aqueous Solution via Seed-Mediated Growth Coupled with Oxidative Etching. Langmuir 2018, 34, 6077–6084.
12. Li, N.; Yin, H.; Zhuo, X.; Yang, B.; Zhu, X.-M.; Wang, J. Infrared-Responsive Colloidal Silver Nanorods for Surface-Enhanced Infrared Absorption. Adv. Opt. Mater. 2018, 6.
13. Sun, Y.; Xia, Y. Shape-Controlled Synthesis of Gold and Silver Nanoparticles. Science 2002, 298, 2176–2179.
14. Tang, B.; An, J.; Zheng, X.; Xu, S.; Li, D.; Zhou, J.; Zhao, B.; Xu, W. Silver Nanodisks with Tunable Size by Heat Aging. J. Phys. Chem. C 2008, 112, 18361–18367.
15. Gunasekaran, S.; Sankari, G.; Ponnusamy, S. Vibrational Spectral Investigation on Xanthine and Its Derivatives—The Ophylline, Caffeine and Theobromine. Spectrochim. Acta A 2005, 61, 117–127.
16. Wiley, B.; Herricks, T.; Sun, Y.; Xia, Y. Polyol Synthesis of Silver Nanoparticles: Use of Chloride and Oxygen to Promote the Formation of Single-Crystal, Truncated Cubes and Tetrahedrons. Nano Lett. 2004, 4, 1733–1739.
17. Wiley, B.; Xiong, Y.; Li, Z.-Y.; Yin, Y.; Xia, Y. Right Bipyramids of Silver: A New Shape Derived from Single Twinned Seeds. Nano Lett. 2006, 6, 765–768.
18. Bryan, W.W.; Jamison, A.C.; Chinwangso, P.; Rittikulsittichai, S.; Lee, T.-C. Preparation of THPC-Generated Silver, Platinum, and Palladium Nanoparticles and their Use in the Synthesis of Ag, Pt, Pd, and Pt/Ag Nanoshells. RSC Adv. 2016, 6, 68150–68159.
19. Pajor-Świerzy, A.; Szczepanowicz, K.; Kamyshny, A.; Magdassi, S. Metallic Core-Shell Nanoparticles for Conductive Coatings and Printing. Adv. Colloid Interface Sci. 2021, 299, 102578.
20. Wiley, B.J.; Chen, Y.; McLellan, J.M.; Xiong, Y.; Li, Z.-Y.; Ginger, A.D.; Xia, Y. Synthesis and Optical Properties of Silver Nanobars and Nanorice. Nano Lett. 2007, 7, 1032–1036.
21. Sun, Y.; Mayers, B.; Herricks, T.; Xia, Y. Crystalline Silver Nanowires by Soft Solution Processing. Nano. Lett. 2003, 3, 955–960.
22. Garcia-Leis, A.; Arreba, I.R.; Sanchez-Cortes, S. Morphological Tuning of Plasmonic Silver Nanostars by Controlling the NanoParticle Growth Mechanism: Application in the SERS Detection of the Amyloid Marker Congo Red. Colloids Surf. A Physicochem. Eng. Asp. 2017, 535, 49–60.

23. Reguera, J.; Langer, J.; de Aberasturi, D.J.; Liz-Marzán, L.M. Anisotropic Metal Nanoparticles for Surface Enhanced Raman Scattering. Chem. Soc. Rev. 2017, 46, 3866–3885.
24. Loiseau, A.; Asila, V.; Boitel-Aullen, G.; Lam, M.; Salmain, M.; Boujday, S. Silver-Based Plasmonic Nanoparticles for and their Use in Biosensing. Biosensors 2019, 9, 78.
25. Wiley, B.J.; Im, S.H.; Li, Z.-Y.; McLellan, J.; Siekkinen, A.; Xia, Y. Maneuvering the Surface Plasmon Resonance of Silver Nanostructures through Shape-Controlled Synthesis. J. Phys. Chem. B 2006, 110, 15666–15675.
26. Xue, C.; Mirkin, C.A. pH-Switchable Silver Nanoprism Growth Pathways. Angew. Chem. 2007, 119, 2082–2084.
27. Jiang, X.C.; Chen, W.M.; Chen, C.Y.; Xiong, S.X.; Yu, A. Role of Temperature in the Growth of Silver Nanoparticles Through a Synergetic Reduction Approach. Nanoscale Res. Lett. 2010, 6, 32–39.
28. Yoo, J.; So, H.; Yang, M.; Lee, K.-J. Effect of Chloride Ion on Synthesis of Silver Nanoparticle Using Retrieved Silver Chloride as a Precursor from the Electronic Scrap. Appl. Surf. Sci. 2019, 475, 781–784.
29. Zhang, Y.; Peng, H.; Huang, W.; Zhou, Y.; Yan, D. Facile Preparation and Characterization of Highly Antimicrobial Colloid Ag or Au Nanoparticles. J. Colloid Interface Sci. 2008, 325, 371–376.
30. Malassis, L.; Dreyfus, R.; Murphy, R.J.; Hough, L.A.; Donnio, B.; Murray, C.B. One-Step Green Synthesis of Gold and Silver Nanoparticles with Ascorbic Acid and their Versatile Surface Post-Functionalization. RSC Adv. 2016, 6, 33092–33100.
31. Leng, Z.; Wu, D.; Yang, Q.; Zeng, S.; Xia, W. Facile and One-Step Liquid Phase Synthesis of Uniform Silver Nanoparticles Reduction by Ethylene Glycol. Optik 2018, 154, 33–40.
32. Sakthivel, P.; Sekar, K. A Sensitive Isoniazid Capped Silver Nanoparticles-Selective Colorimetric Fluorescent Sensor for Hg2+ Ions in Aqueous Medium. J. Fluoresc. 2020, 30, 91–101.
33. Sreelekha, E.; George, B.; Shyam, A.; Sajina, N.; Mathew, B. A Comparative Study on the Synthesis, Characterization, and Antioxidant Activity of Green and Chemically Synthesized Silver Nanoparticles. BioNanoScience 2021, 11, 489–496.
34. Kamarudin, D.; Hashim, N.A.; Ong, B.H.; Hassan, C.R.C.; Manaf, N.A. Synthesis of Silver Nanoparticles stabilised by PVP for Polymeric Membrane Application: A Comparative Study. Mater. Technol. 2021, 1–13.
35. Waqas, M.; Zulfiqar, A.; Ahmad, H.B.; Akhtar, N.; Hussain, M.; Shafiq, Z.; Abbas, Y.; Mehmood, K.; Ajmal, M.; Yang, M. Fabrication of Highly Stable Silver Nanoparticles with Shape-Dependent Electrochemical Efficacy. Electrochim. Acta 2018, 271, 641–651.

36. Makwana, B.A.; Vyas, D.J.; Bhatt, K.D.; Jain, V.K.; Agrawal, Y.K. Highly Stable Antibacterial Silver Nanoparticles as Selective Fluorescent Sensor for Fe3+ Ions. Spectrochim. Acta Part A Mol. Biomol. Spectrosc. 2015, 134, 73–80.
37. Pajor-Świerzy, A.; Farraj, Y.; Kamyshny, A.; Magdassi, S. Air Stable Copper-Silver Core-Shell Submicron Particles: Synthesis and Conductive ink Formulation. Colloids Surf. A Physicochem. Eng. Asp. 2017, 521, 272–280.
38. Raza, M.A.; Kanwal, Z.; Rauf, A.; Sabri, A.N.; Riaz, S.; Naseem, S. Size- and Shape-Dependent Antibacterial Studies of Silver Nanoparticles Synthesized by Wet Chemical Routes. Nanomaterials 2016, 6, 74.
39. Restrepo, C.V.; Villa, C.C. Synthesis of Silver Nanoparticles, Influence of Capping Agents, and Dependence on Size and Shape: A Review. Environ. Nanotechnol. Monit. Manag. 2021, 15, 100428.
40. Jayaramudu, T.; Raghavendra, G.M.; Varaprasad, K.; Reddy, G.V.S.; Reddy, A.B.; Sudhakar, K.; Sadiku, E.R. Preparation and Characterization of Poly (ethylene Glycol) Stabilized Nano Silver Particles by a Mechanochemical Assisted Ball Mill Process. J. Appl. Polym. Sci. 2015, 133.
41. Zhang, H.; Zou, G.; Liu, L.; Tong, H.; Li, Y.; Bai, H.; Wu, A. Synthesis of Silver Nanoparticles Using Large-Area Arc Discharge and Its Application in Electronic Packaging. J. Mater. Sci. 2016, 52, 3375–3387.
42. Mafuné, F.; Kohno, J.-Y.; Takeda, Y.; Kondow, T.; Sawabe, H. Formation and Size Control of Silver Nanoparticles by Laser Ablation in Aqueous Solution. J. Phys. Chem. B 2000, 104, 9111–9117.
43. Munkhbayar, B.; Tanshen, R.; Jeoun, J.; Chung, H.; Jeong, H. Surfactant-Free Dispersion of Silver Nanoparticles into MWCNT-Aqueous Nanofluids Prepared by One-Step Technique and their Thermal Characteristics. Ceram. Int. 2013, 39, 6415–6425.
44. Park, S.; Her, J.; Cho, D.; Haque, M.; Park, J.H.; Lee, C.S. Preparation of Conductive Nanoink Using Pulsed-Wire-Evaporated Copper Nanoparticles for Inkjet Printing. Mater. Trans. 2012, 53, 1502–1506.
45. Song, J.-W.; Lee, D.-J.; Yılmaz, F.; Hong, S.-J. Effect of Variation in Voltage on the Synthesis of Ag Nanopowder by Pulsed Wire Evaporation. J. Nanomater. 2012, 2012, 24.
46. Chung, W.-H.; Hwang, Y.-T.; Lee, S.-H.; Kim, H.-S. Electrical Wire Explosion Process of Copper/Silver Hybrid Nano-Particle Ink and Its Sintering via Flash White Light to Achieve High Electrical Conductivity. Nanotechnology 2016, 27, 205704.
47. Cano-Raya, C.; Denchev, Z.Z.; Cruz, S.F.; Viana, J.C.; Cano-Raya, C.; Denchev, Z.Z.; Cruz, S.F.; Viana, J.C. Chemistry of Solid Metal-Based Inks and Pastes for Printed Electronics—A Review. Appl. Mater. Today 2019, 15, 416–430.

48. Salary, R.; Lombardi, J.P.; Tootooni, M.S.; Donovan, R.; Rao, P.K.; Borgesen, P.; Poliks, M.D. Computational Fluid Dynamics Modeling and Online Monitoring of Aerosol Jet Printing Process. J. Manuf. Sci. Eng. 2016, 139, 021015.
49. Cheon, J.M.; Lee, J.H.; Song, Y.; Kim, J. Synthesis of Ag Nanoparticles Using an Electrolysis Method and Application to Inkjet Printing. Colloids Surf. A Physicochem. Eng. Asp. 2011, 389, 175–179.
50. Kosmala, A.; Wright, R.; Zhang, Q.; Kirby, P. Synthesis of Silver Nano Particles and Fabrication of Aqueous Ag Inks for Inkjet Printing. Mater. Chem. Phys. 2011, 129, 1075–1080.
51. Chen, C.; Dong, T.-Y.; Chang, T.; Chen, M.; Chen, H.; Chen, I. Using Nanoparticles as Direct-Injection Printing Ink to Fabricate Conductive Silver Features on a Transparent Flexible PET Substrate at Room Temperature. Acta Mater. 2012, 60, 5914–5924.
52. Jung, I.; Jo, Y.H.; Kim, I.; Lee, H.M. A Simple Process for Synthesis of Ag Nanoparticles and Sintering of Conductive Ink for Use in Printed Electronics. J. Electron. Mater. 2011, 41, 115–121.
53. Tung, H.-T.; Chen, I.-G.; Kempson, I.M.; Song, J.-M.; Liu, Y.-F.; Chen, P.-W.; Hwang, W.-S.; Hwu, Y. Shape-Controlled Synthesis of Silver Nanocrystals by X-ray Irradiation for Inkjet Printing. ACS Appl. Mater. Interfaces 2012, 4, 5930–5935.
54. Novara, C.; Petracca, F.; Virga, A.; Rivolo, P.; Ferrero, S.; Chiolerio, A.; Geobaldo, F.; Porro, S.; Giorgis, F. SERS Active Silver Nanoparticles Synthesized by Inkjet Printing on Mesoporous Silicon. Nanoscale Res. Lett. 2014, 9, 527.
55. Zhang, N.; Luo, J.; Liu, R.; Liu, X. Tannic Acid Stabilized Silver Nanoparticles for Inkjet Printing of Conductive Flexible Electronics. RSC Adv. 2016, 6, 83720–83729.
56. Liu, Z.; Ji, H.; Wang, S.; Zhao, W.; Huang, Y.; Feng, H.; Wei, J.; Li, M. Enhanced Electrical and Mechanical Properties of a Printed Bimodal Silver Nanoparticle Ink for Flexible Electronics. Phys. Status Solidi A 2018, 215, 1800007.
57. Barrera, N.; Guerrero, L.; Debut, A.; Santa-Cruz, P. Printable Nanocomposites of Polymers and Silver Nanoparticles for Antibacterial Devices Produced by DoD Technology. PLoS ONE 2018, 13, e0200918.
58. Trinh, D.C.; Dang, T.M.D.; Tran, K.H.; Dang, M.C. Preparation of Conductive Ink Based on Silver Nanoparticles. Adv. Nat. Sci. Nanosci. Nanotechnol. 2019, 10, 045007.
59. Hao, Y.; Gao, J.; Xu, Z.; Zhang, N.; Luo, J.; Liu, X. Preparation of Silver Nanoparticles with Hyperbranched Polymers as a Stabilizer for Inkjet Printing of Flexible Circuits. New J. Chem. 2019, 43, 2797–2803.
60. Yang, W.; Mathies, F.; Unger, E.L.; Hermerschmidt, F.; List-Kratochvil, E.J.W. One-Pot Synthesis of a Stable and Cost-Effective Silver Particle-Free Ink for Inkjet-Printed Flexible Electronics. J.

Mater. Chem. C 2020, 8, 16443–16451.

61. Jadav, J.K.; Umrania, V.V.; Rathod, K.J.; Golakiya, B.A. Development of Silver/Carbon Screen-Printed Electrode for Rapid Determination of Vitamin C from Fruit Juices. LWT 2018, 88, 152–158.
62. Liu, L.; Wan, X.; Sun, L.; Yang, S.; Dai, Z.; Tian, Q.; Lei, M.; Xiao, X.; Jiang, C.; Wu, W. Anion-Mediated Synthesis of Monodisperse Silver Nanoparticles Useful for Screen Printing of High-Conductivity Patterns on Flexible Substrates for Printed Electronics. RSC Adv. 2014, 5, 9783–9791.
63. Ding, J.; Liu, J.; Tian, Q.; Wu, Z.; Yao, W.; Dai, Z.; Liu, L.; Wu, W. Preparing of Highly Conductive Patterns on Flexible Substrates by Screen Printing of Silver Nanoparticles with Different Size Distribution. Nanoscale Res. Lett. 2016, 11, 412.
64. Shankar, R.; Groven, L.; Amert, A.; Whites, K.W.; Kellar, J.J. Non-Aqueous Synthesis of Silver Nanoparticles Using Tin Acetate as a Reducing Agent for the Conductive Ink Formulation in Printed Electronics. J. Mater. Chem. 2011, 21, 10871–10877.
65. Ivanov, V.V.; Efimov, A.A.; Myl'Nikov, D.A.; Lizunova, A.A. Synthesis of Nanoparticles in a Pulsed-Periodic Gas Discharge and Their Potential Applications. Russ. J. Phys. Chem. A 2018, 92, 607–612.
66. Sonawane, A.; Mujawar, M.A.; Bhansali, S. Effects of Cold Atmospheric Plasma Treatment on the Morphological and Optical Properties of Plasmonic Silver Nanoparticles. Nanotechnology 2020, 31, 365706.